Implementation of various bed load transport equations at monitoring sites along the Sagavanirktok River

By

Jenah C. Laurio, B.S.

Project Submitted in Partial Fulfillment of the Requirements

for the Degree of

Master of Science

in

Civil Engineering

With a concentration in

Water Resources Engineering

University of Alaska Fairbanks

May 2019

APPROVED BY:

Horacio Toniolo, Committee Chair

Dave Barnes, Committee Member

Svetlana Stuefer, Committee Member

Leroy Hulsey, Department Chair

Department of Civil Engineering

Abstract

In May 2015, the Sagavanirktok River in Alaska flooded, spilling over the Dalton Highway and destroying several sections of the road near the community of Deadhorse. The Alaska Department of Transportation and Public Facilities made repairs to the road and funded the University of Alaska Fairbanks, Water and Environmental Research Center (WERC), to conduct a multiyear study of hydro-sedimentological conditions on the Sagavanirktok River. Personnel from the WERC installed four monitoring stations for research purposes. The first monitoring station (DSS1) is located near Deadhorse at Milepost (MP) 405 of the Dalton Highway, the second (DSS2) is located below the Ivishak River (MP 368), the third (DSS3) is located in Happy Valley (MP 335), and the fourth (DSS4) is located at MP 318. Near each monitoring station, large pits were excavated to trap bed sediment as it moves downstream. Researchers involved in the Sagavanirktok River study have been collecting bathymetry measurements from the sediment pits since fall of 2015.

The following document discusses a research project that focused on bed load transport along the Sagavanirktok River at monitoring sites DSS1, DSS2, and DSS3. Monitoring site DSS4 was not included in this study due to difficulties retrieving sediment data caused by high water levels. Sediment transport volumes measured from the test pits were compared with volume estimations calculated using Acronym (a computer program), and applying the bed load equations of Meyer-Peter and Muller, Wong and Parker, Ashida and Michue, Fernandez Luque and Van Beek, Engelund and Fredsoe, the Parker fit to Einstein's relation, Lajeunesse et al., and Wilson, with a critical Shields value (τ_c^*) of 0.06 and 0.03. The study results showed that in all cases the bed load transport volumes measured at sites DSS2 and DSS3 were far smaller than those calculated using the bed load transport equations. For monitoring site DSS1, a few of the bed load transport equations estimated volumes were close to those measured. The Acronym program was used only for sites DSS2 and DSS3 due to difficulties creating the grain size distribution curve at DSS1. Data show that the volumes calculated by Acronym are greater than those measured at both sites. The bed load transport equations used for the project were not applicable to the Sagavanirktok River.

Acknowledgments

I would like to express my deepest gratitude to my committee chair Dr. Horacio Toniolo for his advice and un-ending patience. Your mentorship and encouragement has played a vital role in the success of this project, and has taught me life lessons that I will carry with me as I move into the next chapter of life. Furthermore, I would like to thank my committee members Dr. Svetlana Stuefer and Dr. David Barnes for their time and insight. Thank you for your advice and for investing in me. I would also like thank Fran. Thank you for setting time aside to look at my document, and to give me great writing advice.

To my family, thank you for encouraging me in all my pursuits. Thank you for pushing me, and constantly reminding me that my job in life is to learn, be joyful, and to care for others. I would also like to thank my Chi-Alpha community for their love and generosity. Thank you for giving me a home away from home, and being my support system here in Fairbanks.

Lastly, I would like to acknowledge my fellow graduate schoolmates. Thank you for walking through these last few years with me, and providing me with free psychology sessions.

Table of Content

List of Figures

List of Tables

1. Introduction

The Dalton Highway in Alaska, formerly known as the Haul Road, was built in 1974. The highway was built to transport material between the Yukon River and Prudhoe Bay during construction of the trans-Alaska pipeline (The Milepost, 2019). The Dalton Highway stretches nearly 414 miles across Alaska; it begins near Fairbanks and ends in Deadhorse (U.S. Department of the Interior, Bureau of Land Management, 2017). Today, the Dalton Highway serves as the only access road to Prudhoe Bay, a major U.S. oil field along the Arctic Ocean (NASA, 2015).

In May 2015 the Sagavanirktok River, which is parallel to the Dalton Highway and the trans-Alaska pipeline, overflowed after an "unseasonably warm spring" (Toniolo et al., 2017). Floodwater from the river spilled over the Dalton Highway, damaging access roads to the Alyeska Pipeline and to the community of Deadhorse (NASA, 2015). After this flooding event, the Alaska Department of Transportation and Public Facilities (ADOT&PF) and the Alyeska Pipeline Service Company (APSC) made repairs to the road and the pipeline, respectively. Working with the University of Alaska Fairbanks, Water and Environmental Research Center (UAF, WERC), the APSC began a long-term monitoring program of the Sagavanirktok River basin, and the ADOT&PF funded a multiyear project related to sediment transport. The ADOT&PF project involved monitoring surface hydro-meteorological conditions before breakup, measuring hydro-sedimentological conditions during breakup and summer, and reviewing historical imagery of the aufeis extent. Researchers from UAF involved in the Sagavanirktok River study (hereafter referred to as the Sag River study) installed four monitoring stations along the west bank of the river: DSS1, DSS2, DSS3, and DSS4. The ADOT&PF excavated seven pits—one at DSS1 and two each at DSS2, DSS3, and DSS4. UAF researchers used the pits to estimate the sediment transport volume through bathymetric survey data comparison. The purpose of the pits was to capture bed sediment as it moved downstream. Volume measurements, taken each summer, were used to determine the total change in volume from 2015–2018.

The sediment transport portion of the Sag River study was divided into two parts: characterizing suspended load and bed load. This report focuses solely on the bed load transport volumes at monitoring sites DSS1, DSS2, and DSS3 from summers of 2016–2018 on the Sag River. Multiple bed load equations and the Acronym computer program were used to estimate

bed load transport volumes. The bed load transport equations used implement a single grain size, whereas the Acronym program applies multiple grain sizes. The estimated values were compared with sediment transport volumes found through bathymetric survey data. Sediment grain size, water slope, hydrographs, and bathymetric survey data collected during the Sag River study were used for this project.

1.1 Bed Load Transport

Sediment in a river is transported as suspended load or bed load. Suspended sediment refers to sediment particles that are brought into suspension (Julien, 2010). Bed load, also known as contact load, refers to sediment particles that maintain contact with the riverbed (Julien, 2010). The bed load equations depend heavily on the Shields parameter, which is a non-dimensional number used to calculate the condition at which a particle will move. The Shields parameter is further discussed in Section 3.2.1.

1.2 Research Objective

The objective of this project was to determine if eight existing bed load transport equations, and the Acronym computer program, could be used to approximate the bed load transport volume in monitoring pits near DSS1, DSS2, and DSS3 during high flow events, from summers of 2016–2018, along the Sag River. The calculated volumes were compared with the measured volumes found through bathymetric survey data.

2. Study Area

The Sag River in Alaska begins in the mountains of the Brooks Range and flows to the Beaufort Sea north of Deadhorse, a service community for Prudhoe Bay (Figure 1). Nearly half of the Sag River basin is within the Ivishak River drainage. The area of the basin is about 13,500 km^2, and is fed by snowmelt, rain, and small glaciers (Toniolo et al., 2017). Since 1983, the discharge of the river has been monitored by the U. S. Geological Survey (USGS) near Pump Station 3 (Milepost [MP] 325) (Toniolo et al., 2017). In 2015, WERC researchers installed four hydro-sedimentological research stations on the west bank of the Sag River. The first monitoring station (DSS1) is located near Deadhorse; the second (DSS2) is located below the Ivishak River; the third (DSS3) is located in Happy Valley; and the fourth (DSS4) is located at MP 318 of the Dalton Highway, as shown in Figure 1. The selected locations represent different channel characteristics (Toniolo et al., 2016). Three of the four hydro-sedimentological research sites—DSS1, DSS2, and DSS3—were included in this project. Monitoring station DSS4 was not included due to difficulties retrieving sediment data caused by high water levels. At each monitoring site, the ADOT&PF attempted to excavate two pits. At research site DSS1, however, only one pit was excavated due to poor access to the dry gravel bar, an area of sediment deposited by the flow of the river. At monitoring sites DSS2 and DSS3, a dry pit and a wet pit were excavated. The dry pits were located at higher elevations from the gravel bar, and the wet pits were located in the active channel where the water was shallow during the time of excavation. The positioning of the two pits reduced the probability that both would fill completely.

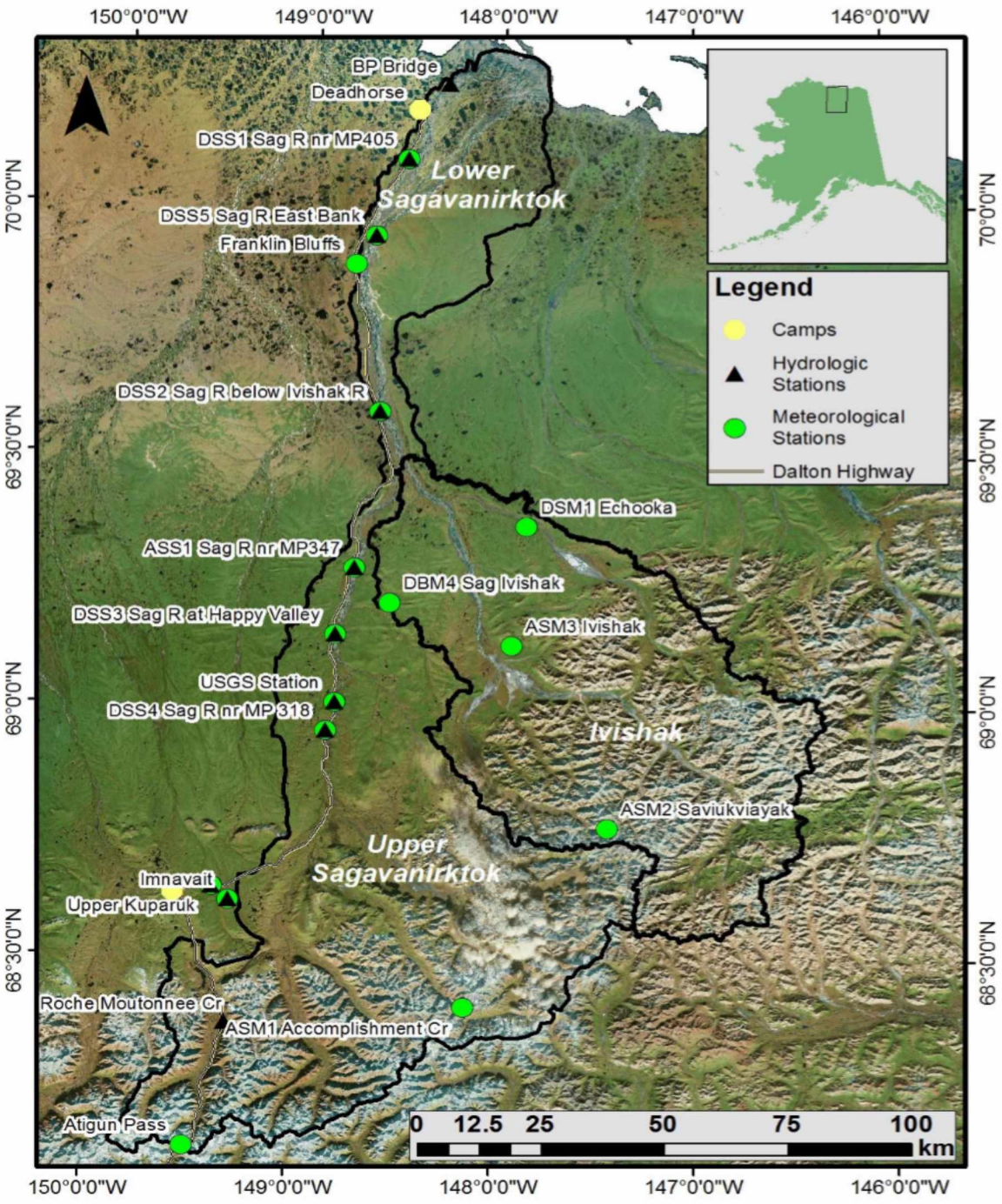

Figure 1: Location of monitoring sites (DSS1, DSS2, DSS3, and DSS4). The thin white line indicates the Dalton Highway, and the black lines show the Sag River watershed boundaries (Toniolo et al., 2018).

Near MP 395 of the Dalton Highway, the Sag River splits into two channels. Monitoring station DSS1 is located close to MP 405, where the river is characterized by braiding and a wide floodplain (Toniolo et al., 2017). Figure 2 shows the location of the test pit near monitoring site DSS1.

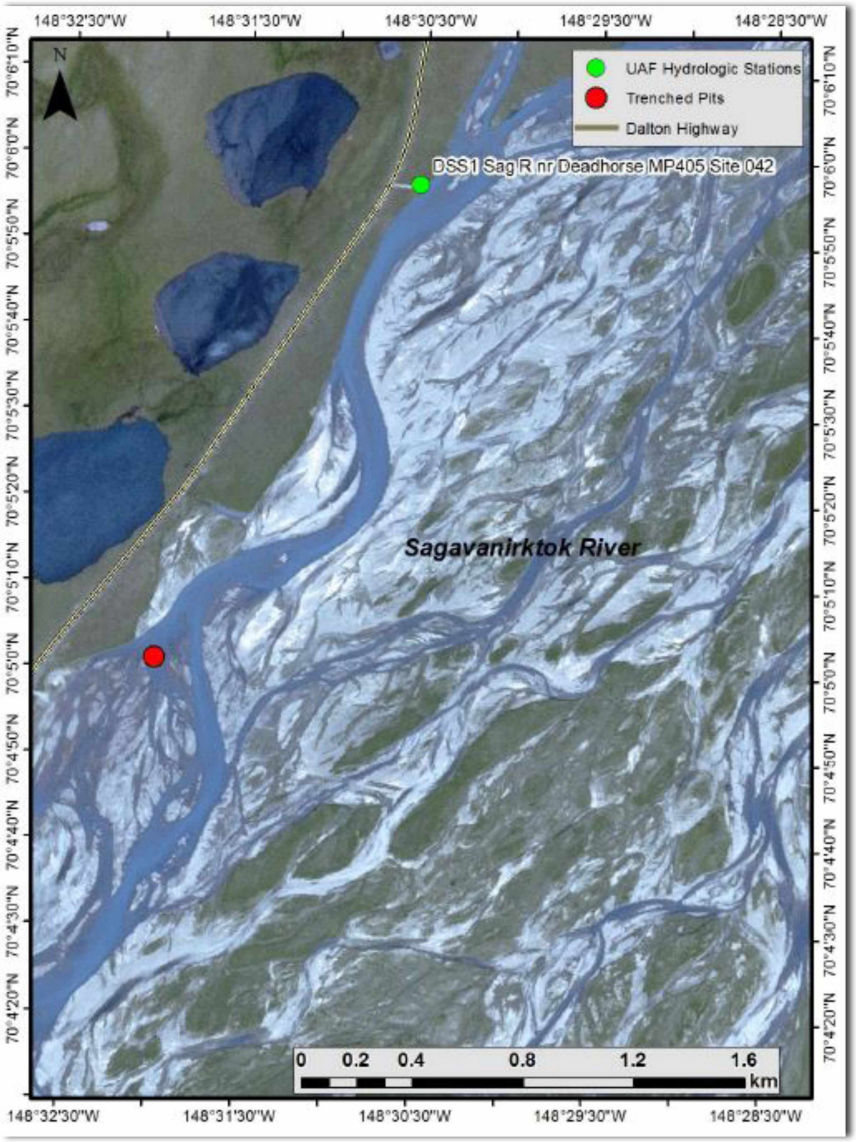

Figure 2: The test pits in the channel of the Sag River at monitoring site DSS1. Only 1 pit was excavated; it is located just over a mile from the monitoring station. The flow direction is from bottom to top (Toniolo et al., 2017).

Monitoring site DSS2 is located near MP 368 of the Dalton Highway, which is below the Ivishak River. The monitoring pits at site DSS2 were excavated on the left side of the channel, where spur dikes, which are structures placed on riverbanks to protect against erosion, were installed to protect the pipeline (Toniolo et al., 2017). Figure 3 shows the location of the pits in the river channel.

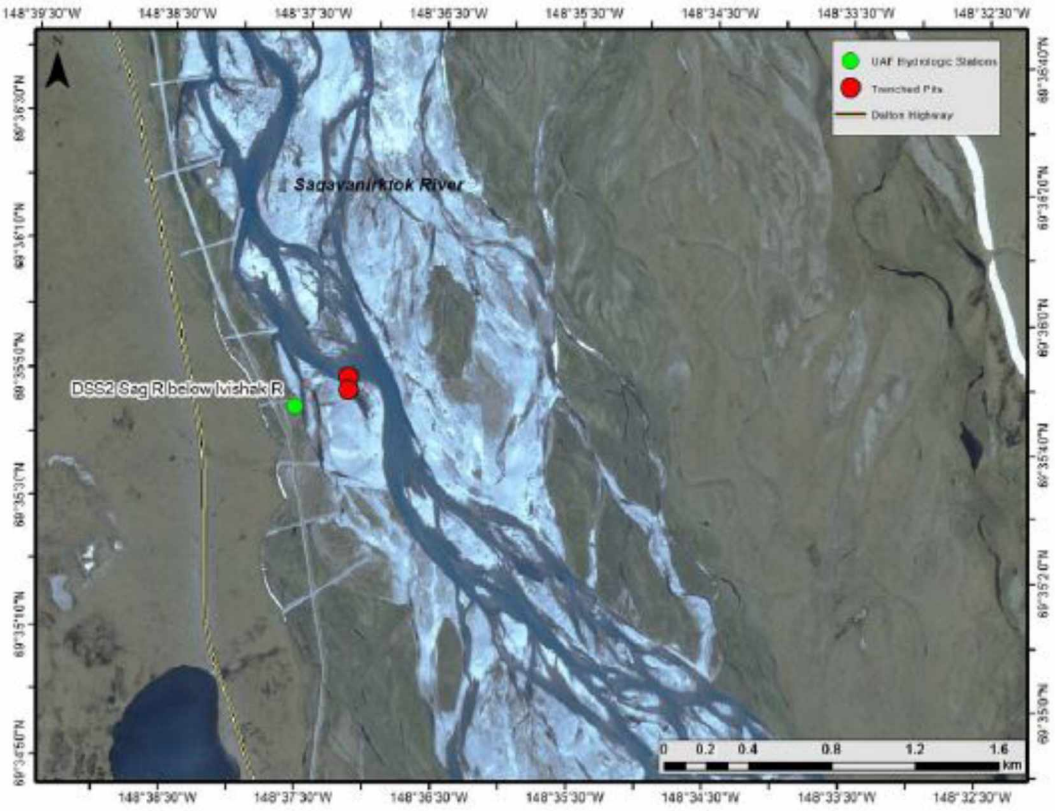

Figure 3: The test pits in the channel of the Sag River at monitoring site DSS2. The flow direction of the river is from bottom to top (Toniolo et al., 2017).

Monitoring site DSS3 is located in Happy Valley near MP 334 of the Dalton Highway. Happy Valley is an active camp and airstrip (Toniolo et al., 2018). The monitoring station was installed on the south end of the runway; the test pits are on the north end of the runway. Figure 4 shows the location of the test pits at DSS4 on the Sag River.

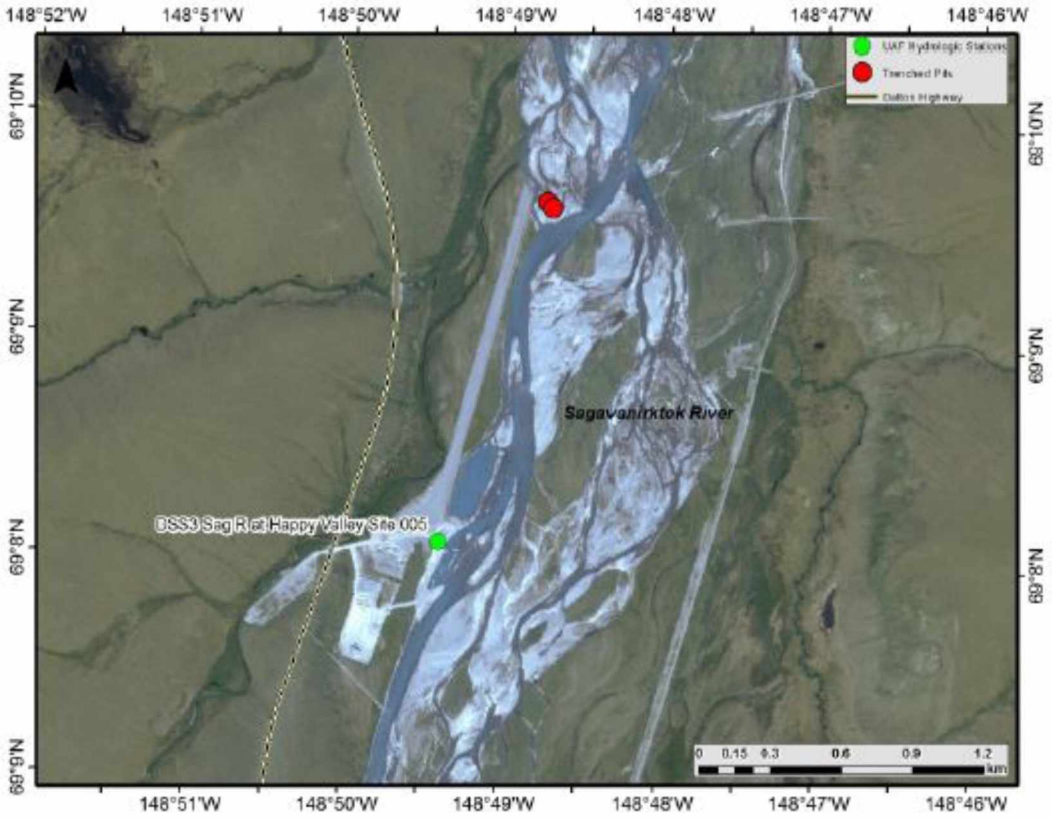

Figure 4: The test pits in the channel of the Sag River at monitoring site DSS3. The monitoring pits are about a mile from the monitoring site. The flow direction is from bottom to top (Toniolo et al., 2017)

3. Methodology

This project involved calculating volumetric sediment deposition in test pits along the Sag River during high flow events from the summers of 2016–2018, using eight bed load transport equations and the Acronym computer program. The results were compared with volume calculations derived from bathymetric survey data retrieved by project personnel.

During the preliminary stages of the project, several methods of assessing bed load transport, such as the utilization of a virtual velocity (McNamara et al., 2008), were investigated. The majority of methods explored were not applicable due to required additional fieldwork.

3.1 Bathymetry

At each monitoring site the test pits were analyzed. For example, at the monitoring pit near research site DSS2, it can be inferred that the total area of the pit had decreased over time (Figures 5 and 6). Topographic tranformations of the test pits caused by sediment deposition and erosion were confirmed by comparing data from bathymetric surveys, which are depth measurements of bodies of water (National Geographic, 2019) (Figure 7).

Figure 5: Dry pit on September 23, 2015, at monitoring site DSS2. Flow direction is from right to left (Toniolo et al., 2017).

Figure 6: Dry pit on July 9, 2017, at monitoring site DSS2. Flow direction is from right to left (Toniolo et al., 2017).

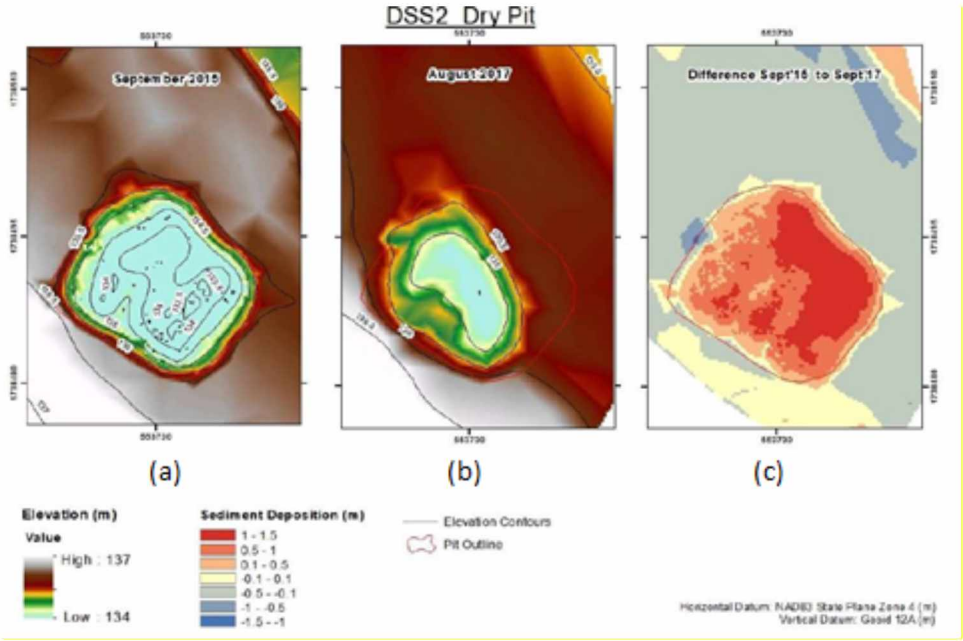

Figure 7: Dry pit bathymetry survey data comparison from 2015 to 2017 (Toniolo et al., 2017).

The change of the volume of the pit from 2015 to 2017 is illustrated in Figure 7. Comparison of the pit size in 2017 (Figure 7b) to the pit size in 2015 (Figure 7a) shows that the pit volume had decreased, meaning sediment deposition had occurred. The volume differences between survey data are shown in Figure 7c.

Figure 8 shows the bathymetry measurements from 2017 to 2018. The yellow line cutting through the center of the pit shows the location of the transect in Figure 9, where change in the pit from 2015 to 2018 is illustrated.

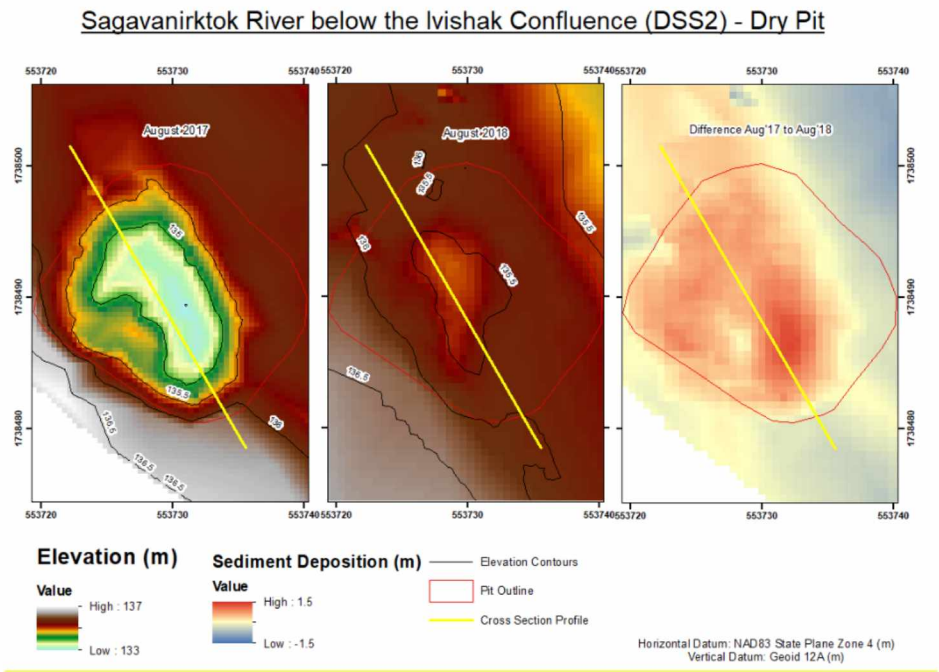

Figure 8: Dry pit bathymetry survey data from 2017 to 2018 (Toniolo et al., 2018)

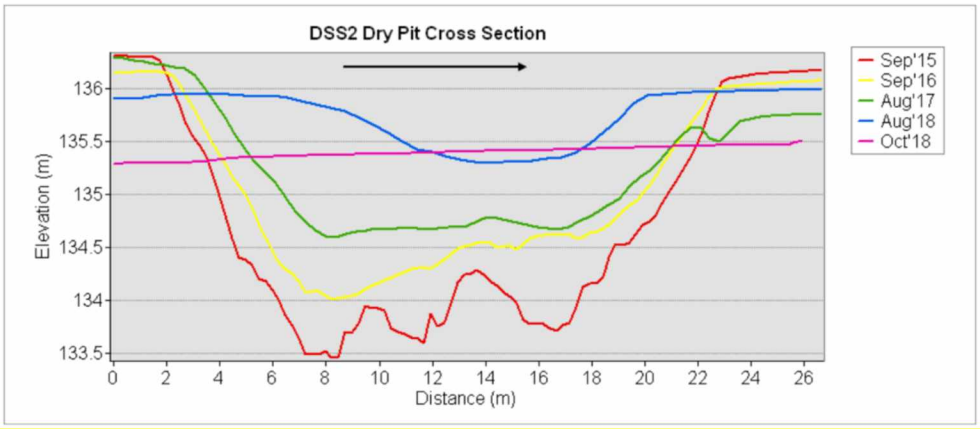

Figure 9: The change in the dry pit from 2015 to 2018 near monitoring site DSS2 (Toniolo et al., 2018).

3.2 Sediment Transport Equations

Several of the bed load transport equations used for the project were compiled from an article published in 2010, which discusses an experimental investigation of bed load sediment of uniform grain size under steady turbulent flow (Lajeunesse et al., 2010). Bed load equations require the use of the Shields non-dimensional parameter and the critical Shields value. The Acronym computer program, which implements a sediment grain size distribution to estimate

bed load transport, was developed in 2004 (Parker, 2004); it is dependent on the Parker (1990) surface-based bed load transport relation (Parker, 1990), which is further discussed in Section 3.3.

3.2.1 Shields parameter

The fluid flow around sediment particles exerts forces, which can cause the initiation of motion (Julien, 2010). The Shields parameter (τ^*) is a non-dimensional value used to determine conditions in which sediment will move; it is the ratio of shear force to bed particle weight, which is the resisting force of non-cohesive material (Julien, 2010). The Shields parameter is a function of shear velocity (u_*), submerged specific density of sediment (R), gravity (g), and mean sediment diameter (D_{50}).

Shields Parameter:

$$\tau^* = \frac{u_*^2}{RgD} \tag{1}$$

In the bed load transport calculations performed during the project, published critical Shields values (τ_c^*) were used.

3.2.2 Shear velocity

The dimensionless sediment transport rate per unit width (q^*) relies on eight parameters; fluid density (ρ), sediment density (ρ_s), kinematic viscosity of water (υ), gravity (g), water slope (S), mean diameter (D_{50}), flow depth (H), and shear velocity (u_*), where τ is shear stress (γHS) and γ is the specific weight of water. Water slope measurements and sediment samples, which were used to find the mean grain size, were collected in the field at each site. The flow depth values for each high flow event were calculated from the relationship discussed in Section 3.2.3.

Shear velocity:

$$u_* = \left(\frac{\tau}{\rho}\right)^{\frac{1}{2}} \tag{2}$$

3.2.3 Flow depth

Average flow depth measurements (Figure 10) derived from discharge readings were used to create a unique mathematical association between stage and water depth for each

monitoring site. The relationship was used to predict flow depth at any given time during high flow events, which were determined through analyzing hydrograph data. Figure 11 shows an example of a partial hydrograph from summer of 2016 at monitoring site DSS2.

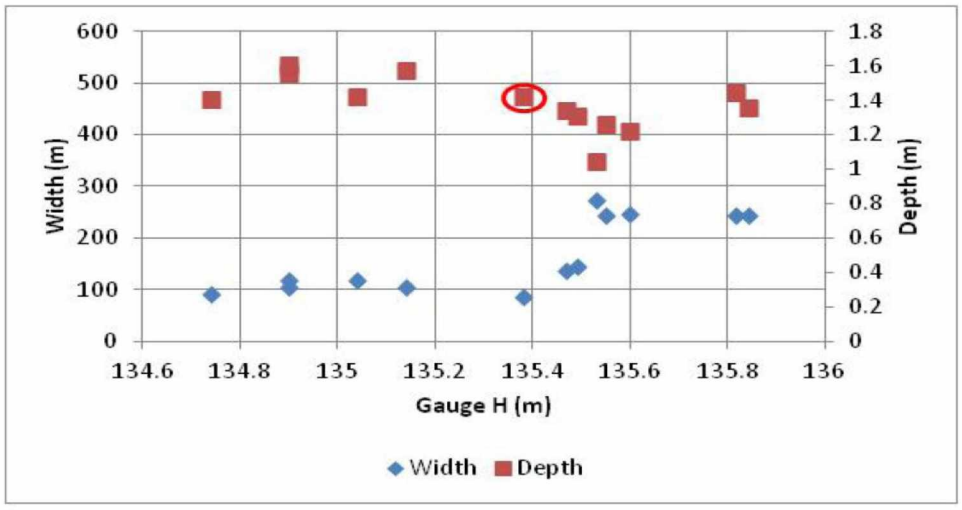

Figure 10*:* Flow depth measurements collected during summers 2015–2018 from monitoring site DSS2 (Toniolo et al., 2018).

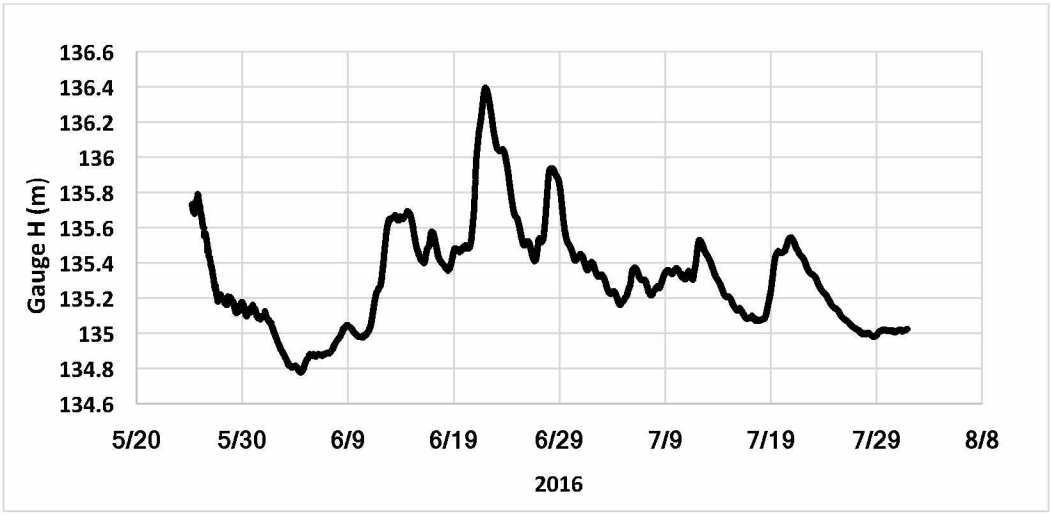

Figure 11: Stage and date data from monitoring site DSS2 during the months of June and July 2016.

Figure 12 shows a simplified section of the partial hydrograph from monitoring site DSS2 in 2016 (Figure 11), where high flow events took place. Figure 13 shows the flow depths corresponding to gauge height after the mathematical relationship between flow depth and gauge had been applied.

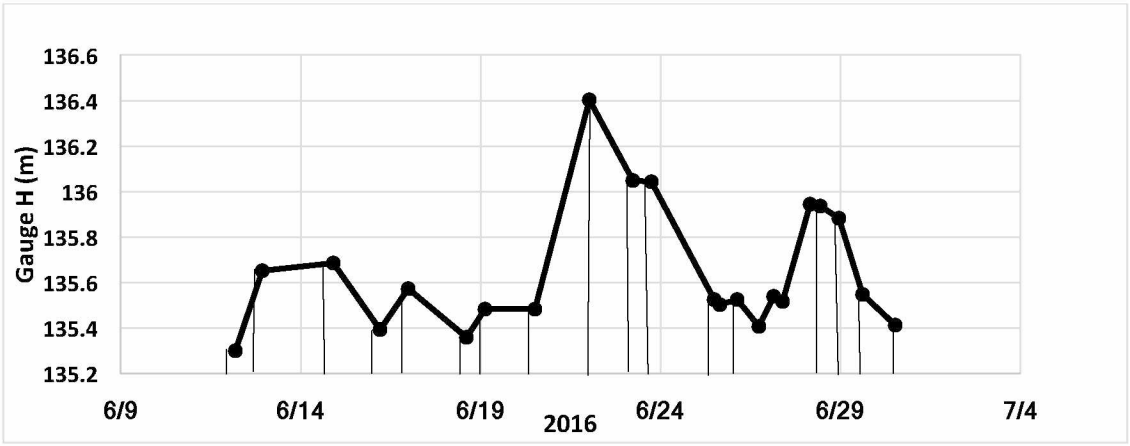

Figure 12: Sample of the hydrograph section used for the sediment transport equations for monitoring site DSS2.

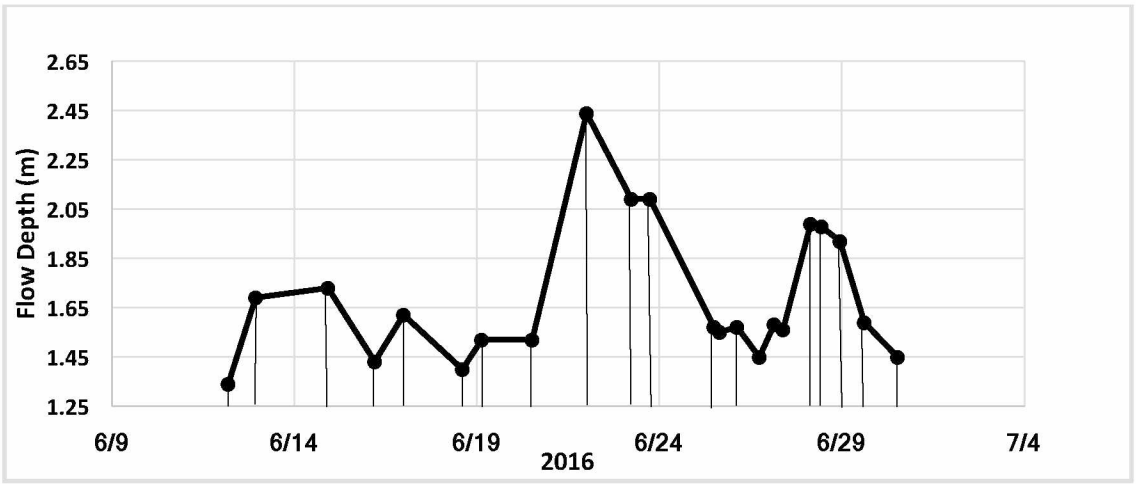

Figure 13: Sample of hydrograph section where the relationship between gauge and flow depth was used.

The flow depth values derived from gauge data were used to calculate shear stress at any given point on the hydrograph. The time differences between flow depth values, along with pit width measurements, were used to calculate the average bed load transport per unit width.

3.2.4 Dimensionless sediment transport equations

The mechanisms of bed load transport are not completely understood (Fernandez Luque, and Van Beek, 1976). The majority of the equations used in bed load transport are purely empirical, such as the Shields formula, or contain underlying theory based on assumptions not fully justified (Fernandez Luque, and Van Beek, 1976). Several bed load transport equation assessments have been made in various rivers within the last few decades, but no formula has

performed consistently well (Lopez et al., 2014). Many of the bed load transport equations used for the project were derived from natural streams such as Oak Creek (Parker, 1990), from lab work (Meyer-Peter and Muller, 1948), and from data re-analysis (Wong and Parker, 2006).

The most commonly used bed load transport equations, as reported by Lajeunesse et al. (2010), are as follows:

Meyer-Peter and Muller (1948)):

$$q^* = 8(\tau^* - \tau_c^*)^{\frac{3}{2}} \qquad \tau_c^* = 0.047 \tag{3}$$

Wong and Parker (2006):

$$q^* = 3.97(\tau^* - \tau_c^*)^{\frac{3}{2}} \qquad \tau_c^* = 0.0495 \tag{4}$$

Ashida and Michiue (1973):

$$q^* = 17(\tau^* - \tau_c^*)(\tau^{*\frac{1}{2}} - \tau_c^{*\frac{1}{2}}) \qquad \tau_c^* = 0.05 \tag{5}$$

Fernandez Luque and Van Beek(1976):

$$q^* = 5.7(\tau^* - \tau_c^*)^{\frac{3}{2}} \qquad \tau_c^* = 0.045 \tag{6}$$

Engelund and Fredsoe (1976):

$$q^* = 18.74(\tau^* - \tau_c^*)(\tau^{*\frac{1}{2}} - (0.7 * \tau_c^{*\frac{1}{2}})) \qquad \tau_c^* = 0.05 \tag{7}$$

Lajeunesse, Malverti, and Charru (2010):

$$q^* = 10.6(\tau^* - \tau_c^*)\left(\tau^{*\frac{1}{2}} - \tau_c^{*\frac{1}{2}} + 0.25\right) \tag{8}$$

$$\mathrm{D} = 1.15 \quad \tau_c^* = 0.016 \pm 0.03$$

$$\mathrm{D} = 2.24 \quad \tau_c^* = 0.023 \pm 0.002$$

$$\mathrm{D} = 5.50 \quad \tau_c^* = 0.037 \pm 0.001$$

Additional equations reported in Parker (2004) are as follows:

Wilson (1966):

$$q^* = 12(\tau^* - \tau_c^*)^{\frac{3}{2}} \tag{9}$$

$$\tau_c^* = 0.03, \tau_c^* = 0.06$$

Parker, 1978, fit to relation of Einstein, 1950:

$$q^* = 11.2(\tau^*)^{\frac{3}{2}}\left(1 - \frac{\tau_c^*}{\tau^*}\right)^{4.5} \tag{10}$$

$$\tau_c^* = 0.03$$

3.2.5 Dimensional sediment transport rate

The calculated Shields parameter was used in each of the bed load transport equations shown in Section 3.2.4, where a dimensionless sediment transport (q^*) rate was calculated.

To find the dimensional sediment transport (q_s) rate per unit width, the following equation was used.

Dimensional Sediment Transport Rate (Lajeunesse et al., 2010)

$$q_s = q^*(RgD^3)^{\frac{1}{2}} \tag{11}$$

As mentioned in Section 3.2.3, flow depth measurements were calculated for any given time on a hydrograph. To find the volume (V) of sediment transport, the dimensional sediment transport rate (Eq. 11) was multiplied by the pit width (B) and the duration of time in between

flow depth values. The total bed load transport volume for each high flow event was found through the summation of the sediment transport volumes calculated between flow depth measurements (Appendix B).

$$V = (q_s)(time)(B) \tag{12}$$

3.3 Acronym

The equations in Section 3.2.3 use a single grain size to estimate the bed load transport rate. The Acronym program calculates the sediment transport rate considering multiple grain sizes. The program implements Parker's surface-based bed load transport relation. The parameters used in the bed load transport relation are presented below (Parker, 1990):

τ_b=*boundary shear stress on the bed*

$u_*=(\tau_b/\rho)^{.5}$=*shear velocity on the bed*

q_{bi}=*total volume of gravel bed load transport per unit width of grains in size range*

p_i=*fraction of gravel bed load in the grain size rang e*

F_i=*fraction in the surface layer*

W_i^*=*transport relation*

Transport Relation (Parker, 2004):

$$W_i^* = \frac{Rgq_{bi}}{F_{iU_*^3}} \tag{13}$$

To use the program, the specific gravity of sediment, the shear velocity of flow, and the grain size distribution (with a minimum of 2 mm) were input. The sediment transport relation predicted the total volume of bed load transport per unit width of the material, as well as the grain size distribution of the load (Parker, 1990). For monitoring sites DSS2 and DSS3, a grain size distribution curve was used to find grain sizes at 90, 70, 50, and 30% finer. A grain size distribution curve for DSS1 could not be created due to high water levels, preventing the research team from retrieving sediment grain size samples.

3.4 Porosity

Porosity (p) is the ratio of the volume of voids (Vv) to the total volume (V_T). Table 1 shows estimations of porosity values for different soils from the Unified Soil Classification

System (USCS). The "GW-GP" porosity values were used based on the type of gravel present in the Sag River (Geotechdata.info, 2013). By using the maximum porosity of 0.38 and the minimum porosity of 0.23, the volume of sediment alone was calculated (Zurich, 1999).

The sediment volume (Vs) was found through the following equation:

$$V_S = \frac{V_V - (pV_V)}{p} \tag{14}$$

Table 1: Porosity values for different USCS soil types (Geotechdata.info 2013)

Description	USCS	Porosity [-]		
		min	max	Specific value
Well graded gravel, sandy gravel, with little or no fines	GW	0.21	0.32	
Poorly graded gravel, sandy gravel, with little or no fines	GP	0.21	0.32	
Silty gravels, silty sandy gravels	GM	0.15	0.22	
Gravel	(GW-GP)	0.23	0.38	
Clayey gravels, clayey sandy gravels	GC	0.17	0.27	
Glatial till, very mixed grained	(GC)	-	-	0.20
Well graded sands, gravelly sands, with little or no fines	SW	0.22	0.42	
Coarse sand	(SW)	0.26	0.43	
Fine sand	(SW)	0.29	0.46	
Poorly graded sands, gravelly sands, with little or no fines	SP	0.23	0.43	
Silty sands	SM	0.25	0.49	
Clayey sands	SC	0.15	0.37	
Inorganic silts, silty or clayey fine sands, with slight plasticity	ML	0.21	0.56	
Uniform inorganic silt	(ML)	0.29	0.52	

4. Results and Discussion

The results from the bed load transport equations, the Acronym computer program, and the measured values found from the bathymetric survey data for monitoring sites DSS1, DSS2, and DSS3 are presented in Tables 2, 3, and 4. The maximum and minimum porosity values 0.38 and 0.23 were used to evaluate the measured sediment volumes (Section 3.4).

4.1 Bed Load Transport Analysis for Sediment Pit near Monitoring Site DSS1

For monitoring site DSS1, high flow events from 2016 and 2018 were analyzed. In 2017, there was no significant change in the sediment pit volume. The Acronym computer program was not used for DSS1 due to difficulties retrieving samples to create a sediment grain size distribution.

The calculated volume change (from the bathymetric survey data) for 2016 was 140 m^3, while the closest bed sediment volume predicted by the equations was 138 m^3, given by the Engelund and Fredsoe equation (7). The measured values, applying porosities of 0.23 and 0.38, were 108 m^3 and 87 m^3, respectively.

From June 21 to July 5, 2018, the bed sediment volume closest to the measured volumes was 39 m^3, using the Wong and Parker equation (2). The measured volumes, with porosity values of 0.23 and 0.38, were 45 m^3 and 36 m^3, respectively. In September 2018, the smallest bed load transport volume calculated was 436 m^3, using the Ashida and Michue equation (5). The measured volumes, however, did not exceed 45 m^3.

There were a few instances where the data appeared to be within the same range; but no consistent trends exist.

Table 2: Sediment transport volume estimated using bed load equations, the Acronym computer program, and bathymetric data for monitoring site DSS1.

Results Summary Table (DSS1)			
Wet/Dry	Wet	Wet	Wet
Year	2016	2018	2018
Date	6/12–6/30	6/21–7/5	9/1–9/10
Volume (m^3)			
Meyer-Peter/Muller	319	237	1,736
Wong/Parker	26	39	576
Ashida/Michue	10	21	436
Fernandez-Luque/Van Beek	432	314	1,525
Engelund/Fredsoe	138	196	2,347
Wilson ($\tau_c^* = 0.06$)	0	0	0
Wilson ($\tau_c^* = 0.03$)	5,392	11,102	12,389
Lajeunesse/Malverti/Charru	1,501	914	2,210
Parker/ Einstein	703	431	1,192
Measured volume (m^3)			
Year	2016	2018	2018
Measured vol. w/o porosity	140	58	58
Porosity (0.23)	108	45	45
Porosity (0.38)	87	36	36

4.2 Bed Load Transport Analysis for Sediment Pits near Monitoring Site DSS2

For monitoring site DSS2, results from the bed load transport equations suggest that bed sediment within the range of 2,000 m^3 to 36,000 m^3 was transported in summer 2016, from June 12 to June 30. The Acronym computer program calculated a sediment transport volume of 5,062 m^3. The volume measurements calculated through bathymetric survey data for the wet pit were 105 m^3 and 84 m^3, with porosity values of 0.23 and 0.38, respectively. The dry pit measurement results showed sediment volumes of 97 m^3, with a porosity of 0.23, and 78 m^3, with a porosity of 0.38. The bed sediment volumes calculated using the bed load transport equations and the Acronym computer program were far greater than the measured values. This result was found for the dry pits in 2017 and 2018 as well.

In 2017, the wet pit at monitoring site DSS2 filled completely with sediment (Toniolo et al., 2017); therefore, measurements were not available for 2017 and 2018. A theoretical minimum sediment transport value of 4,400 m^3 was calculated using the Wong and Parker

equation (2), and 3,903 m^3 was calculated using the Acronym computer program for 2017. In 2018, the minimum theoretical value of 2,854 m^3 was found using the Wilson equation (9), and 2,798 m^3 was estimated using the Acronym computer program.

Table 3: Sediment transport volume estimated by the bed load equations, the Acronym computer program, and bathymetric data for monitoring site DSS2.

Results Summary Table (DSS2)						
Wet/Dry	Wet	Dry	Wet	Dry	Wet	Dry
Year	2016		2017		2018	
Date	6/12–6/30		7/23–7/28		6/19–6/26	
Volume (m^3)						
Meyer-Peter/Muller	17,691	24,060	9,588	13,039	9,420	12,811
Wong/Parker	7,774	10,572	4,400	5,983	4,217	5,735
Ashida/Michue	11,964	16,271	7,871	10,705	6,656	9,053
Fernandez-Luque/Van Beek	13,505	18,367	7,148	9,721	7,117	9,679
Engelund/Fredsoe	26,395	35,897	14,725	20,026	14,096	19,171
Wilson ($\tau_c^* = 0.06$)	2,170	2,951	9,150	12,444	2,854	3,881
Wilson ($\tau_c^* = 0.03$)	14,366	19,538	22,581	30,710	9,513	12,938
Lajeunesse/Malverti/Charru	15,532	21,123	8,223	11,183	8,053	10,953
Parker/Einstein	11,773	16,011	7,051	9,590	6,266	8,521
Acronym	5,062	6,884	3,903	5,308	2,798	3,805
Measured (m^3)						
Year	2016		2017		2018	
Wet/Dry	Wet	Dry	Wet	Dry	Wet	Dry
Measured vol. w/o porosity	136	126		23		84
Porosity (0.23)	105	97		18		65
Porosity (0.38)	84	78		14		52

4.3 Bed Load Transport Analysis for Sediment Pits near Monitoring Site DSS3

The results from monitoring site DSS3 indicate that volume estimations made from the bed load transport equations were far greater than those calculated by the Acronym computer program. Acronym results ranged from 433 m^3 to 1,197 m^3, whereas the bed load transport equation results ranged from 1,765 m^3 to 33,684 m^3. In 2017, there was no significant change in

the dry pit volume. The Acronym computer program results suggested that 526 m^3 of bed sediment was transported into the pit, and the bed load transport equations showed a minimum of 3,258 m^3, using the Wong and Parker equation (2). Also, in 2018 the wet pit showed no change in measured values, but the Acronym computer program and the Wong and Parker equation (2) computed values of 1,197 m^3 and a minimum transport volume of 1,863 m^3, respectively.

In 2016, the volume computed for the wet pit using the Acronym computer program was 457 m^3, and the volume measured was 49 m^3 (porosity of 0.23). In all other cases, the Acronym results were far greater than the measured volumes.

Table 4: Sediment transport volume estimated by the bed load equations, the Acronym computer program, and bathymetric data for monitoring site DSS3.

Results Summary Table (DSS3)						
Wet/Dry	Wet	Dry	Wet	Dry	Wet	Dry
Year	2016		2017		2018	
Date	6/20–7/2		7/20–8/11		8/17–9/7	
Volume (m^3)						
Meyer-Peter/Muller	6,603	6,256	8,511	8,063	4,261	4,037
Wong/Parker	2,830	2,681	3,439	3,258	1,863	1,765
Ashida/Michue	3,922	3,716	4,430	4,197	2,903	2,750
Fernandez-Luque/Van Beek	5,106	4,838	6,788	6,431	3,264	3,092
Engelund/Fredsoe	9,688	9,178	12,277	11,630	6,350	6,016
Wilson ($\tau_c^* = 0.06$)	3,781	3,587	3,678	3,484	3,090	2,927
Wilson ($\tau_c^* = 0.03$)	20,819	19,723	33,684	31,911	12,670	12,003
Lajeunesse/Malverti/Charru	5,867	5,558	8,242	7,808	3,801	3,601
Parker/Einstein	4,127	3,910	5,420	5,134	2,884	2,732
Acronym	457	433	555	526	1,197	1,134
Measured (m^3)						
Year	2016		2017		2018	
Wet/Dry	Wet	Dry	Wet	Dry	Wet	Dry
Measured vol. w/o porosity	64	21	52			46
Porosity (0.23)	49	16	40			35
Porosity (0.38)	40	13	32			29

4.4 Discussion

The results show that the majority of the volumes calculated using bed load transport equations and the Acronym computer program were significantly larger than the volumes measured. Although the degree of discrepancy in the data may appear fairly large, it is not uncommon for such results to occur (Lopez et al., 2014).

The bed load transport equations used for the project were dependent on variables such as the Shields parameter and shear velocity, which is a function of shear stress. The shear stress value in a river can vary greatly along a river reach, and is generally dependent on the geometry of a channel (slope and water depth). The shear stress values calculated for the project were a function of the water slope collected from field data, and a relationship created between flow depth and gauge height from discharge measurements taken from the summers of 2015–2018.

The results also show that in some cases the sediment transport equations and the Acronym computer programs calculated sediment transport when no sediment deposition had occurred.

Turbulence in different environments, and sediment characteristics, such as shape and size distribution, unique to individual rivers, played a large role in the substantial differences between the results from the measured values and the results from the bed load transport equations. The wide range of values used for the critical Shields parameter in the bed load transport equations also contributed to the discrepancies in the results.

5. Conclusions and Recommendations

The purpose of this project was to determine if bed load transport equations and the Acronym computer program could be used to characterize the bed load transport conditions in monitoring pits near research stations DSS1, DSS2, and DSS3.

Field data collected from the research sites by project personnel were used to determine the mean diameter of sediment and the water slope, and to solve for flow depth at any given time on a hydrograph. The flow depth values derived from the relationship between gauge and flow depth were used to calculate shear stress during high flow events in the summers of 2016–2018. The Shields parameter equation, which is a function of shear velocity, was then used in each bed load transport equation. The bed load transport equations assumed a single grain size (D_{50}), and the Acronym computer program was used to calculate the bed load transport volume where multiple grain sizes were obtained.

The volumes calculated were compared with volumes that were measured, using bathymetric survey data from 2015–2018. The volumes calculated using the bed load transport equations were far greater than the measured volumes. Although a few volumes calculated using the bed load equations were comparable to the measured volumes, they were not consistent for each site. The Acronym computer program results were also greater than those measured. Neither the bed load transport equations nor the Acronym computer program appear to be a reliable method for characterizing bed load transport conditions near the monitoring sites along the Sag River. The reality of sediment transport estimation is that it is a difficult and daunting task. It is unlikely that a single sediment transport equation is viable for every river.

Modeling the conditions of the Sag River in a large flume (considering all scaling issues) would provide a better understanding of the threshold of sediment movement for the grain size specific to the Sag River.

Developing an equation unique to the Sag River would be the most reliable method of better representing the bed load transport conditions along the river reach. Adjusting the Sag River equation to each individual site would also mitigate errors, and provide a more reliable estimation of bed load transport.

References

Ashida, K., and Michiue, M. (1973). Studies on bed load transport rate in open channel flows, in Proceedings of the International Association for Hydraulic Research International Symposium on River Mechanics, 9-12 January 1973, Bangkok, Thailand, pp. 407–417, Asian Inst. of Technol., Bangkok.

Engelund, F., and Fredsoe, J. (1976). A sediment transport model for straight alluvial channels, *Nord. Hydrol.*, 7(5), 293–306.

Fernandez Luque, R., and Van Beek, R. (1976). Erosion and Transport of Bed Load Sediment. *Journal of Hydraulic Research,* 14(2), 127–144, DOI: 10.1080/00221687609499677

Geotechdata.info (2013) Soil Porosity. Retrieved on February 8, 2019 from *http://geotechdata.info/parameter/soil-void-ratio.html.*

Julien, P. Y. (2006). *River Mechanics.* Cambridge: Cambridge University. Press.

Julien, P. Y. (2010). *Erosion and Sedimentation.* Cambridge: Cambridge University Press.

Lajeunesse, E., Malverti L., Charru,F. (2010). Grain scale: Experiments and modeling. *Journal of Geophysical Research: Earth Surface*, 115(4). https://doi.org/10.1029/2009JF001628

López, R., Vericat, D., and Batalla, R. J. (2014). Evaluation of bed load transport formulae in a large regulated gravel bed river. *Journal of Hydrology,* 510, 164–181. http://dx.doi.org/10.1016/j.jhydrol.2013.12.014

McNamara, J. O., Oatley, J. A., Kane, D. L., and Hinzman, L. D. (2008). Case study of a large summer flood on the North Slope of Alaska: Bedload transport. *Hydraulogy Research,* 39, 299–308.

Meyer-Peter, E., and Muller, R. (1948). Formulas for Bed-Load Transport. *International Association for Hydro-Environmental Engineering and Research, Int. Assoc. for Hudraul. Res., Stockholm*

NASA (National Aeronautics and Space Administration) (2015). Flooding of Dalton Highway. Retrieved February 8, 2019 from https://earthobservatory.nasa.goc/image/85905/flooding-of-dalton-highway

National Geographic Society (2018). Bathymetry. Retrieved on February 6, 2019. from https://www.nationalgeographic.org/encylopedia/bathymetry/

Parker, G. (1979). Hydraulic geometry of active gravel rivers. *Journal of Hydraulic Engineering*, 105(9), 1185-1201.

Parker, G. (1990). Surface-base bedload transport relation for gravel rivers. *Journal of Hydraulic Research,* 28(4), 417–436

Parker, G. (1990). The "ACRONYM" series of Pascal programs for computing bedload transport in gravel rivers. *Externam Memorandum M-220. St. Anythony Falls Hydraulic*

Parker, G. (2004). Sediment Transport Mophodynamics with application to rivers and turbidity Currents. *[Power Point Slides].*

Shields, A., (1936). Anwendung der Ähnlichkeitsmechanik auf die Geschiebebewegung*: Berlin, Preussische Versuchanstalt für Wasserbau und Schiffbau, Mitteilungen, no. 26, 25*
Laboratory, University of Minnesota.

The Milepost (2019). Dalton Highway. Morris Media. Retrieved February 2019 from https://www.themilepost.com/highways/dalton-highway/

Toniolo, H., Tschetter, T., Tape, K. D., Cristobal, J., Youcha, E. K., Schnabel, W. E., Vas, D., and Keech, J. (2016). Hydro-sedimentological Monitoring and Analysis for Material Sites on the Sagavanirktok River 2015-2016 Data Report.

Toniolo, H., Youch, E. K., Tape, K. D., Paturi, R., Homan, J., Boudurant, A., Landes, I., Laurio, J., Vas, D., Keech, J., Tschetter, T., and LaMesjerant, E. (2017). Hydrological, Sedimentological, and Meteorological Observations and Analysis on the Sagavanirktok River 2017 Interim Report.

Toniolo, H., Youcha, E. K., Tape, K. D., Paturi, R. , Homan, J. , Boudurant, A., LaMesjerant, E., Landes, I., Vas, D., Keech, J., and Laurio, J. (2018). Hydrological, Sedimentological, and Meteorological Observations and Analysis on the Sagavanirktok River 2018 Interim Report.

U.S. Department of the Interior, Bureau of Land Management (2017). Dalton Highway Visitors Guide 2017, 6–7. Retrieved from https://www.blm.gov/visit/dalton-highway

Wilson, K. C. (1966). Bed load transport at high shear stresses. *Journal of Hydraulic Engineering,* 92(6), 49–59.

Wong, M., and Parker, G. (2006). Reanalysis and correction of bed load relation of Meyer-Peter and Muller using their own database. *Journal of Hydraulic Engineering,* 132. https://doi.org/10.1061/(ASCE)0733-9429(2006)132:11(1159)

Zurich (1999). Swiss Standard SN 670 010b:Characteristic Coefficients of Soils. *Association of Swiss Road Traffic Engineering*

Symbols

q^* = dimensionless sediment transport rate	$[-]$
q_s = sediment transport rate per unit width	$[\frac{L^2}{T}]$
τ^* = Shields Parameter	$[-]$
τ^*_{crit} = critical Shields value	$[-]$
τ = shear stress	$[\frac{F}{L^2}]$
γ = specific weight of water	$[\frac{F}{L^3}]$
H = flow depth	$[L]$
B = pit width	$[L]$
S = Slope of water	$[-]$
R =submerged specific density of quartz	$[-]$
g = gravity	$[\frac{L}{T^2}]$
D = diameter of the sediment	$[L]$
u_* = shear velocity	$[\frac{L}{T}]$
Re_s = Settling Reynolds number	$[-]$
ρ_s = density of the sediment	$[\frac{M}{L^3}]$
ρ = density of water	$[\frac{M}{L^3}]$
υ = kinematic viscosity of water	$[\frac{L^2}{T}]$

q_{bi}=total volume of gravel bed load transport per unit width of grains in size range $[\frac{L^2}{T}]$

p_i=fraction of gravel bed load in the grain size range $[-]$

F_i=fraction in the surface layer $[-]$

W_i^*=transport relation $[-]$

Appendix A Acronym program

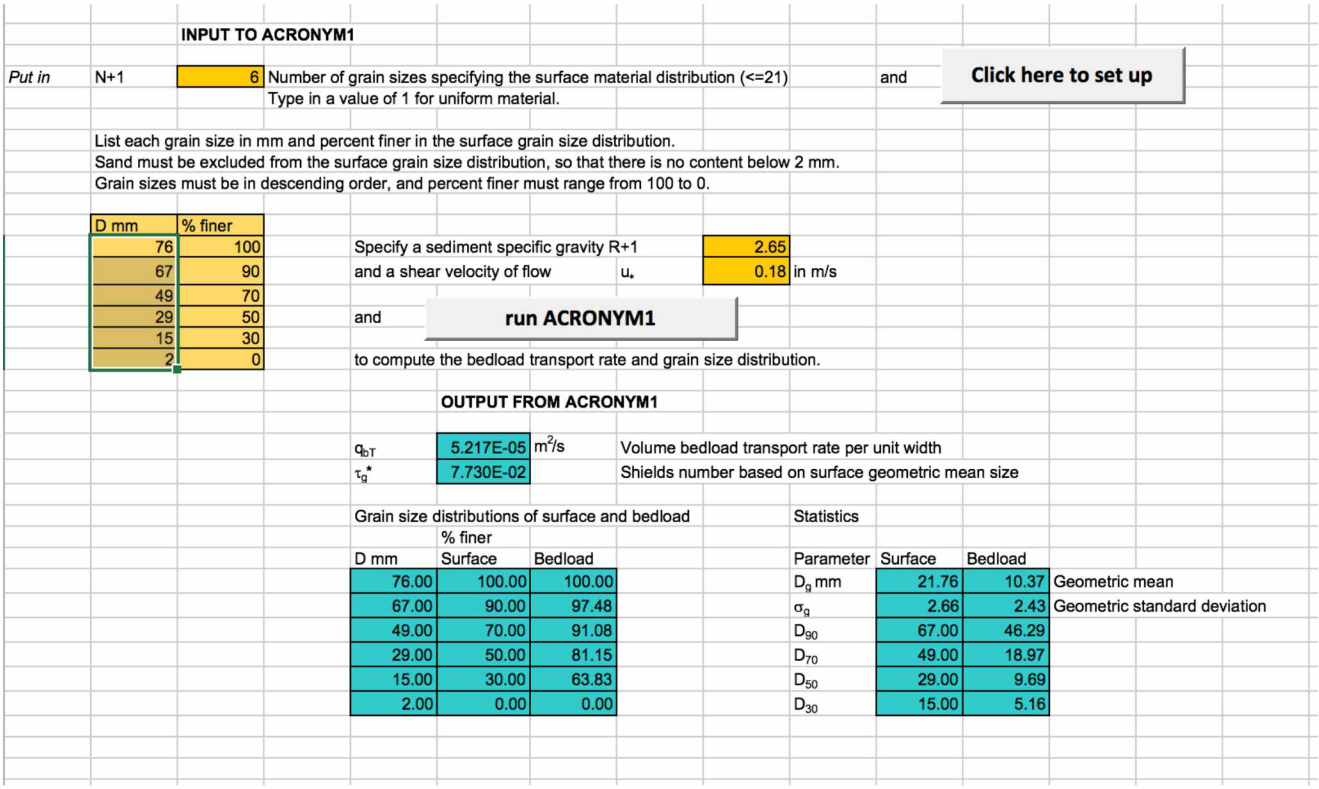

INPUT TO ACRONYM1

Put in N+1 | 6 | Number of grain sizes specifying the surface material distribution (<=21) | and | Click here to set up

Type in a value of 1 for uniform material.

List each grain size in mm and percent finer in the surface grain size distribution.
Sand must be excluded from the surface grain size distribution, so that there is no content below 2 mm.
Grain sizes must be in descending order, and percent finer must range from 100 to 0.

D mm	% finer
76	100
67	90
49	70
29	50
15	30
2	0

Specify a sediment specific gravity R+1 = 2.65

and a shear velocity of flow u_* = 0.18 in m/s

and run ACRONYM1

to compute the bedload transport rate and grain size distribution.

OUTPUT FROM ACRONYM1

q_{bT}	5.217E-05	m^2/s	Volume bedload transport rate per unit width
τ_g^*	7.730E-02		Shields number based on surface geometric mean size

Grain size distributions of surface and bedload

D mm	% finer Surface	Bedload
76.00	100.00	100.00
67.00	90.00	97.48
49.00	70.00	91.08
29.00	50.00	81.15
15.00	30.00	63.83
2.00	0.00	0.00

Statistics

Parameter	Surface	Bedload	
D_g mm	21.76	10.37	Geometric mean
σ_g	2.66	2.43	Geometric standard deviation
D_{90}	67.00	46.29	
D_{70}	49.00	18.97	
D_{50}	29.00	9.69	
D_{30}	15.00	5.16	

Figure A1: The Acronym program is shown. The orange boxes indicate input values

Appendix B: Bed load equation

Q(m^3/s)	
Diamater	0.03
Slope	0.0012
density of Sediment	2650
Kinemaitc Viscosity of water	0.000001
Specific weight	9810
Density of water	1000
Width	16.5
Porosity	1 Still need to find the correct value

Number	Flow Depth	Shear Stress	Shear Velocity	Settling Velocity	Settling Reynolds	Reynolds	Shields Parameter	Time
1	1.5	17.658	0.132883408	0.696846468	20905.39404	20905.39404	0.036363636	0
2	2.07	24.36804	0.156102659	0.696846468	20905.39404	20905.39404	0.050181818	65700
3	2.11	24.83892	0.15760368	0.696846468	20905.39404	20905.39404	0.051151515	170700
4	1.81	21.30732	0.145970271	0.696846468	20905.39404	20905.39404	0.043878788	111000
5	2	23.544	0.153440542	0.696846468	20905.39404	20905.39404	0.048484848	68400
6	1.78	20.95416	0.144755518	0.696846468	20905.39404	20905.39404	0.043151515	139800
7	1.9	22.3668	0.149555341	0.696846468	20905.39404	20905.39404	0.046060606	44700
8	1.9	22.3668	0.149555341	0.696846468	20905.39404	20905.39404	0.046060606	120000
9	1.77	20.83644	0.144348329	0.696846468	20905.39404	20905.39404	0.042909091	29400
10	2.09	24.60348	0.156854965	0.696846468	20905.39404	20905.39404	0.050666667	83700
11	2.13	25.07436	0.158348855	0.696846468	20905.39404	20905.39404	0.051636364	33300
12	2.03	23.89716	0.154587063	0.696846468	20905.39404	20905.39404	0.049212121	69000
13	2.05	24.1326	0.155346709	0.696846468	20905.39404	20905.39404	0.04969697	16500
14	2.03	23.89716	0.154587063	0.696846468	20905.39404	20905.39404	0.049212121	35100
15	1.84	21.66048	0.147174998	0.696846468	20905.39404	20905.39404	0.044606061	180900
16	1.83	21.54276	0.146774521	0.696846468	20905.39404	20905.39404	0.044363636	45900
17	1.79	21.07188	0.145161565	0.696846468	20905.39404	20905.39404	0.043393939	44400
18	1.83	21.54276	0.146774521	0.696846468	20905.39404	20905.39404	0.044363636	34800
19	1.82	21.42504	0.146372948	0.696846468	20905.39404	20905.39404	0.044121212	24900
20	1.97	23.19084	0.15228539	0.696846468	20905.39404	20905.39404	0.047757576	52200
21	1.98	23.30856	0.152671412	0.696846468	20905.39404	20905.39404	0.048	29400
22	1.94	22.83768	0.151121408	0.696846468	20905.39404	20905.39404	0.047030303	61500
23	1.77	20.83644	0.144348329	0.696846468	20905.39404	20905.39404	0.042909091	121800

B1: Shields parameter equation sheet. The red boxes indicate input values.

t*crit	0.047						
Total Volume (m^3)	318.9568933						
Meyer-Peter-Muller							
Equation Used:	8*((t*-tcrit)^(3/2))					Width	Porosity
Shields Parameter	Dimensionless	Dimensional	Volume per unit time			16.5	1
			Hours	*Seconds*		*Volume*	*Volume/Unit Width m^3*
0.036363636	0	0		65700		0.986045051	16.26974334
0.050181818	0.00143583	3.00166E-05		170700		6.380143724	105.2723714
0.051151515	0.002139932	4.47361E-05		111000		2.482854495	40.96709916
0.043878788	0	0		68400		0.327263568	5.399848874
0.048484848	0.000457734	9.56911E-06		139800		0.668880802	11.03653323
0.043151515	0	0		44700		0	0
0.046060606	0	0		120000		0	0
0.046060606	0	0		29400		0	0
0.042909091	0	0		83700		1.55399978	25.64099636
0.050666667	0.001776222	3.71326E-05		33300		1.497338826	24.70609063
0.051636364	0.002525551	5.27976E-05		69000		2.421836123	39.96029604
0.049212121	0.000832345	1.74005E-05		16500		0.336802741	5.557245222
0.04969697	0.00112048	2.34241E-05		35100		0.716471285	11.8217762
0.049212121	0.000832345	1.74005E-05		180900		1.573875216	25.96894106
0.044606061	0	0		45900		0	0
0.044363636	0	0		44400		0	0
0.043393939	0	0		34800		0	0
0.044363636	0	0		24900		0	0
0.044121212	0	0		52200		0.09101814	1.501799307
0.047757576	0.000166813	3.48729E-06		29400		0.129006875	2.128613438
0.048	0.000252982	5.28869E-06		61500		0.163485177	2.697505422
0.047030303	1.3345E-06	2.78983E-08		121800		0.001699005	0.028033587
0.042909091	0	0					

Figure B2: Bed load transport calculation sheet (Meyer-Peter and Muller).

Appendix C: Data used in the bed load transport equations and Acronym Program

Table C1: Data used for 6/12-6/30 2016 DSS1

date	Gauge (m)	H (m)	DT (sec)
6/12/16 15:30	25.30	1.50	0
6/13/16 9:45	25.65	2.07	65700
6/15/16 9:10	25.69	2.11	170700
6/16/16 16:00	25.39	1.81	111000
6/17/16 11:00	25.58	2.00	68400
6/19/16 1:50	25.36	1.78	139800
6/19/16 14:15	25.48	1.90	44700
6/20/16 23:35	25.48	1.90	120000
6/21/16 7:45	25.35	1.77	29400
6/22/16 7:00	25.67	2.09	83700
6/22/16 16:15	25.71	2.13	33300
6/23/16 11:25	25.61	2.03	69000
6/23/16 16:00	25.63	2.05	16500
6/24/16 1:45	25.61	2.03	35100
6/26/16 4:00	25.42	1.84	180900
6/26/16 16:45	25.41	1.83	45900
6/27/16 5:05	25.37	1.79	44400
6/27/16 14:45	25.41	1.83	34800
6/27/16 21:40	25.40	1.82	24900
6/28/16 12:10	25.55	1.97	52200
6/28/16 20:20	25.56	1.98	29400
6/29/16 13:25	25.52	1.94	61500
6/30/16 23:15	25.35	1.77	121800

Table C2: Data used for 6/21-7/5 2018 DSS1

date	Gauge (m)	H(m)	DT (sec)
6/21/18 14:45	25.57	1.99	0
6/21/18 23:00	25.59	2.01	29700
6/22/18 6:10	25.58	2.00	25800
6/22/18 13:10	25.54	1.96	25200
6/22/18 15:25	25.56	1.98	8100
6/22/18 21:30	25.68	2.10	21900
6/23/18 3:15	25.54	1.96	20700
6/23/18 6:15	25.64	2.06	10800
6/23/18 7:10	25.60	2.02	3300
6/23/18 9:10	25.65	2.07	7200
6/23/18 14:25	25.64	2.06	18900
6/23/18 16:10	25.64	2.06	6300
6/23/18 17:25	25.68	2.10	4500
6/23/18 22:35	25.69	2.11	18600
6/24/18 4:15	25.75	2.17	20400
6/24/18 7:40	25.68	2.10	12300
6/24/18 13:30	25.77	2.19	21000
6/26/18 14:05	25.52	1.94	174900
6/27/18 2:20	25.50	1.92	44100
6/28/18 8:10	25.57	1.99	107400
6/28/18 14:30	25.52	1.94	22800
6/29/18 5:20	25.54	1.96	53400
6/29/18 23:45	25.48	1.90	66300
6/30/18 8:50	25.50	1.92	32700
7/1/18 4:00	25.43	1.85	69000
7/1/18 15:05	25.44	1.86	39900
7/2/18 4:10	25.40	1.82	47100
7/2/18 12:40	25.43	1.85	30600
7/3/18 2:00	25.39	1.81	48000
7/3/18 12:00	25.45	1.87	36000
7/3/18 21:50	25.42	1.84	35400
7/4/18 9:45	25.44	1.86	42900
7/5/18 2:40	25.42	1.84	60900

Table C3: Data used for 9/1-9/10 2018 DSS1

date	Gauge (m)	H(m)	DT (sec)
9/1/18 20:00	25.41	1.83	0
9/2/18 4:10	26.00	2.42	29400
9/2/18 15:15	26.04	2.46	39900
9/4/18 6:50	25.75	2.17	142500
9/5/18 5:00	26.01	2.43	79800
9/5/18 21:35	25.95	2.37	59700
9/7/18 7:15	25.97	2.39	121200
9/10/18 9:20	25.52	1.94	266700

Table C4: Data used for 6/12-6/30 2016 DSS2

date	Gauge (m)	H(m)	DT (sec)
6/12/16 4:30	135.30	1.34	0
6/12/16 22:45	135.65	1.69	65700
6/14/16 22:10	135.69	1.73	170700
6/16/16 5:00	135.39	1.43	111000
6/17/16 0:00	135.58	1.62	68400
6/18/16 14:50	135.36	1.40	139800
6/19/16 3:15	135.48	1.52	44700
6/20/16 12:35	135.48	1.52	120000
6/22/16 0:30	136.40	2.44	129300
6/23/16 5:35	136.05	2.09	104700
6/23/16 18:00	136.05	2.09	44700
6/25/16 12:00	135.53	1.57	151200
6/25/16 15:50	135.51	1.55	13800
6/26/16 3:20	135.53	1.57	41400
6/26/16 17:55	135.41	1.45	52500
6/27/16 3:42	135.54	1.58	35220
6/27/16 9:35	135.52	1.56	21180
6/28/16 3:45	135.95	1.99	65400
6/28/16 10:45	135.94	1.98	25200
6/28/16 23:00	135.88	1.92	44100
6/29/16 14:50	135.55	1.59	57000
6/30/16 12:40	135.41	1.45	78600

Table C5: Data used for 7/23-7/28 2017 DSS2

date	Gauge (m)	H(m)	DT (sec)
7/23/17 8:50	135.49	1.53	0
7/23/17 10:50	135.94	1.98	7200
7/24/17 21:00	135.98	2.02	123000
7/25/17 8:30	136.38	2.42	41400
7/25/17 19:00	136.50	2.54	37800
7/28/17 13:45	135.49	1.53	240300

Table C6: Data used for 6/19-6/26 2018 DSS2

date	Gauge (m)	H(m)	DT (sec)
6/19/18 11:05	135.57	1.61	0
6/19/18 19:40	135.72	1.76	30900
6/20/18 9:15	135.74	1.78	48900
6/21/18 0:00	135.94	1.98	53100
6/21/18 17:30	135.99	2.03	63000
6/22/18 6:15	135.91	1.95	45900
6/22/18 19:30	135.97	2.01	47700
6/23/18 9:00	135.89	1.93	48600
6/24/18 7:15	136.07	2.11	80100
6/25/18 11:20	135.72	1.76	101100
6/26/18 12:40	135.57	1.61	91200
6/26/18 16:50	135.58	1.62	15000

Table C7: Data used for 6/20-7/2 2016 DSS3

date	Gauge (m)	H(m)	DT (sec)
6/20/16 3:00	289.15	1.04	0
6/20/16 13:00	289.23	1.12	36000
6/20/16 19:40	289.26	1.15	24000
6/21/16 10:40	289.51	1.40	54000
6/21/16 14:15	289.48	1.37	12900
6/21/16 16:50	289.54	1.43	9300
6/22/16 1:00	289.56	1.45	29400
6/22/16 21:55	289.40	1.29	75300
6/23/16 9:30	289.40	1.29	41700
6/24/16 10:40	289.31	1.20	90600
6/24/16 17:55	289.30	1.19	26100
6/25/16 6:15	289.24	1.13	44400
6/25/16 15:20	289.28	1.17	32700
6/26/16 7:00	289.17	1.06	56400
6/26/16 17:30	289.24	1.13	37800
6/27/16 1:55	289.20	1.09	30300
6/27/16 15:30	289.44	1.33	48900
6/28/16 4:00	289.48	1.37	45000
6/29/16 6:20	289.27	1.16	94800
6/29/16 15:15	289.24	1.13	32100
6/30/16 2:10	289.16	1.05	39300
6/30/16 14:00	289.25	1.14	42600
7/1/16 5:50	289.13	1.02	57000
7/1/16 15:35	289.22	1.11	35100
7/2/16 5:20	289.12	1.01	49500
7/2/16 13:54	289.15	1.04	30840
7/2/16 23:30	289.06	0.95	34560

Table C8: Data used for 7/20-8/11 2017 DSS3

date	Gauge (m)	H(m)	DT (sec)
7/20/17 7:30	289.17	1.06	0
7/21/17 16:30	289.66	1.55	118800
7/22/17 16:30	289.27	1.16	86400
7/24/17 0:00	289.26	1.15	113400
7/25/17 11:00	289.17	1.06	126000
7/30/17 3:45	288.80	0.94	405900
7/30/17 21:15	289.17	1.06	63000
7/31/17 3:00	289.88	1.77	20700
8/2/17 9:15	289.41	1.30	195300
8/4/17 20:30	289.77	1.66	213300
8/6/17 3:30	289.54	1.43	111600
8/6/17 17:45	289.73	1.62	51300
8/11/17 10:30	289.67	1.56	405900

Table C9: Data used for 8/17-9/7 2018 DSS3

date	Gauge (m)	H(m)	DT (sec)
8/17/18 8:07	288.81	0.96	0
8/17/18 21:05	289.17	1.06	46680
8/21/18 11:45	289.08	1.00	312000
8/22/18 18:05	289.29	1.18	109200
43335.64792	289.56	1.45	77280
8/27/18 22:48	288.87	0.98	371700
43344.25208	288.98	0.99	371700
43344.89236	288.97	0.99	55320
9/3/18 16:45	288.81	0.96	156000
9/4/18 13:25	289.21	1.10	74400
9/5/18 6:00	289.08	1.00	59700
9/5/18 16:08	289.23	1.12	36480
9/6/18 4:15	288.81	0.96	43620
9/6/18 16:02	288.81	0.96	42420
9/7/18 17:35	289.17	1.06	91980

Table C10: Pit information

	DSS1	DSS2	DSS3
Width-Wet(m)	16	12.5	9.5
Width-Dry(m)		17	9
Slope	0.0012	0.0022	0.0032
Diameter(m)	0.030	0.030	0.033